Research Article

Congnan Peng, Qian Zhang, Jian-an Liu, Zhen-peng Wang, Zhen-wen Zhao, Ning Kang, Yuxin Chen, and Qing Huo*

Study on titanium dioxide nanoparticles as MALDI MS matrix for the determination of lipids in the brain

https://doi.org/10.1515/gps-2021-0056
received April 28, 2021; accepted August 16, 2021

Abstract: The structures of lipids are diverse, and thus, lipids show various biological functions. Systematic determination of lipids in organisms has always been a concern. In this paper, a methodology on the matrix-assisted laser desorption ionization mass spectrometry (MALDI MS), with titanium dioxide nanoparticles (TiO_2 NPs) as the matrix, was studied for lipid determination. The results showed that the following conditions were preferable in the determination of small-molecule lipids (such as hypoxanthine, guanosine, uridine, and cytidine), lipid standards (such as GC, GM, TG, phosphatidylethanolamine, phosphatidylcholine, and ceramide), and mixed lipids (extracted from brain homogenate with methanol alone and with the B&D method): TiO_2 NPs as the matrix, absolute ethanol as the solvent, 1 mg of TiO_2 NPs dispersed in 1 mL of absolute ethanol as the matrix solution, NaCl as the ionization reagent, and positive mass spectrometry (MS) as the mode. Modified TiO_2 NP as a new matrix for MALDI MS will be a future research direction; in addition, the characteristics of TiO_2 NPs make it a potential matrix for imaging MS.

Keywords: TiO_2 NPs, MALDI mass spectrometry, lipid

1 Introduction

The diversity of lipid structures endows lipids with various biological functions [1]. Lipids are indispensable in the regulation of physiological activities, and the metabolism abnormalities of lipids cause many diseases such as chronic inflammation, atherosclerosis, hypertension, diabetes, obesity, Alzheimer's disease, and cancer [2–4]. Lipids have diversified categories and complex structures, and the different numbers of carbon atoms or unsaturated bonds in lipid acyl chains will diversify lipids into many types and subtypes [5]. Therefore, the systematic determination of lipids in organisms has always been a difficult problem. In recent years, many methods have been developed for lipids detection, such as thin-layer chromatography, liquid chromatography [6], gas chromatography, enzyme-linked immunosorbent assay, nuclear magnetic resonance spectrometry, and mass spectrometry (MS) [7–9]. Among them, MS has been widely applied because it has the advantages of high sensitivity, specificity, high throughput, and high accuracy. The utilization of high-resolution mass detectors has greatly improved the ability of MS for lipid determination and promotes the research on lipids [10,11].

Lipids are the main components of the brain and perform many important functions. Brain nerve cells contain a large amount of 22 carbon hexanoic acid (DHA), and it plays an important role in the development of children's brain nerves [12]. Cholesterol metabolism, lipoprotein (a), apolipoprotein ApoE, etc., are all importantly related to Alzheimer's disease and dementia [13]. A European study showed that a lipid-containing diet can delay or prevent the occurrence of Alzheimer's disease and other dementias. A lipid diet containing Omega-3 fatty acids can inhibit the above-mentioned diseases [14]. Basic and clinical studies have shown that there is an important link between metabolic disorders such as cholesterol, fatty acids and lipids, and the pathogenesis of

* **Corresponding author: Qing Huo,** Biochemical Engineering College of Beijing Union University, Department of Biomedicine, 100023 Beijing, China, e-mail: shthuoqing@buu.edu.cn
Congnan Peng, Qian Zhang, Ning Kang, Yuxin Chen: Biochemical Engineering College of Beijing Union University, Department of Biomedicine, 100023 Beijing, China
Jian-an Liu, Zhen-peng Wang, Zhen-wen Zhao: Institute of Chemistry, Chinese Academy of Sciences, Beijing Mass Spectrum Center, 100190 Beijing, China

stroke [15]. Studying the metabolism of fatty acid endogenous compounds in the brain tissue during the course of ischemic stroke found that: There are 9 fatty acid metabolism abnormalities in the brain tissue of rats with focal cerebral ischemia, 9-hexadecenoic acid, docosa, hexaenoic acid, arachidonic acid, 9-octadecenoic acid, hexadecanoic acid, 11-octadecenoic acid, octadecanoic acid, 13-eicosene acid, 11-eicosenoic acid, can be used as potential biomarkers [16].

Matrix-assisted laser desorption mass spectrometry (MALDI MS) is a new MS technique [17–19]. Typically, a sample is dispersed in matrix molecules and forms crystals. When the crystals are irradiated by laser, the energy derived and accumulated leads to a rapid temperature increase, which sublimates the matrix crystals. The sample and matrix will expand and migrate into the gas phase, the matrix provides the volume flow, in this process, the energy passes on to the sample and ionized it into ions, then the ions are separated and analyzed in the MS system [20,21]. It is noteworthy that monocharged ions are dominant in MALDI, so the signals of ions in these mass spectra can match with the mass of polypeptides and proteins exclusively [22–24].

The laser wavelength of a commercial MALDI apparatus has been fixed already, and thereby the matrix is the most important factor affecting the detection ability of the apparatus. Common matrix materials include solid, liquid and liquid/solid biphasic materials [25–27]. Divided by the chemical properties, matrix materials include inorganic materials such as graphite and metal salts and organic materials (acidic, basic, and neutral) [28,29]. Currently, no matrix is suitable for the analysis of all samples, so the research and analysis of the matrix are very important.

The screening and selecting of the specific matrix are very tricky in MALDI analysis. To be considered as a good matrix, it should satisfy these requirements:

(1) To reduce the force between molecules and prevent the formation of molecular clusters, the matrix should be miscible with the target.
(2) The matrix is stable under vacuum conditions.
(3) The matrix can absorb laser light.
(4) Under laser light, the matrix can protect the sample and transfer energy to it without destroying the sample's structure.
(5) The matrix can provide protons, which can promote the ionization of the sample [30–32]. Because of the uneven distribution of combined matrix-sample crystals on the MALDI target, the reproducibility of samples is poor, especially in the quantitative analysis of MALDI, which is also a difficult problem.

In the presence of traditional organic matrix materials, such as α-cyano-4-hydroxycinnamic acid (CHCA), 2,4,6-trihydroxyacetophenone (THAP), and 2,5-dihydroxybenzoic acid (DHB), the mass spectrum signals of analytes can be intensive. But, because the molecular weights of matrix materials are close to 200 Da, copious matrix debris with a small mass number will be generated when the samples are subjected to laser irradiation. The mass spectrum signals of debris will seriously interfere with the spectral analysis of small molecules. The authors attempted to develop a new matrix material to eliminate debris and simplify the spectrum for more accurate detection of small molecules. Currently, the research and development of nanomaterials are at the cutting edge in the MALDI-TOF MS matrix field [33,34]. Nanomaterial is a new material with a structural unit size of 1–100 nm. Due to its small particle size, large specific surface area, and strong modifiability, it has been widely applied in pharmaceuticals, catalysis, sensing, magnetic recording, and so on. The nanomaterials as the MALDI-TOF MS matrix principally include metal–organic frameworks, carbon-based nanomaterials, silicon-based nanomaterials, metal particles and their oxides, etc.:

(1) Metal–organic framework matrix: Currently, the metal centers of MOFs used to prepare the matrix principally include Zr, Cr, Zn, Cu, etc., and most of the ligands are polyhydroxycarboxylic acids and pyridines, and other organic compounds containing multiple auxochromes and chromophores [35,36].
(2) Nanographene matrix: This matrix includes graphene, graphene derivatives, and their composites. Many different types of graphene derivatives and composites such as graphene sheets [37], grapheme/SiO_2 nanocomposites [38], and *N*-doped graphene [39], have been proven to be excellent MALDI-TOF MS matrixes.
(3) Carbon nanotube matrix: The surface of carbon nanodot can be modified with abundant carboxylic acid groups, showing water solubility and so it can be evenly dispersed in the solution without discharge and pollution. In addition, the size of a carbon nanodot is small (~3 nm), and the analyte is easy to desorb, so the detection limit can be as low as 0.2 fmol [40,41].
(4) Silicon-based nanomaterial matrix: Li et al. [42] prepared a novel MALDI matrix material by the electrochemical etching of porous silicon (PSi), and the surface of the matrix was modified with palladium nanoparticles (Pd NPs). This material can specifically enrich peptides. Due to the limitation of pore size and molecular filtration effect of PSi, the peptides in serum samples could be selectively captured and enriched in the pores, thus eliminating the interference

of large protein molecules in subsequent MALDI-TOF MS detection.

(5) Metal nanoparticle matrix: Co, Ag, Mo, and nanooxides such as TiO_2 and ZrO_2·Fe_3O_4/TiO_2 [43] and ZnO–CuO nanoparticles [44] have been used as the matrix for MALDI-TOF MS to detect small molecules. Functionalization and modification of metal nanomaterials are an important means to improve the performance of the metal nanomaterial matrix [45].

Compared with other biomolecules, lipids have the following characteristics:

(1) The molecular weights (<1,500 U) are low and mass/charge ratios are similar, so the signals may overlap with the relevant peaks of the matrix system in MALDI-MS. This is detrimental to the recognition of phospholipids.
(2) The water solubility is low, and the lipids should be dissolved in the solvent to a certain extent during measurements.
(3) Diverse molecular structures. For example, according to the polar head, the lipids can be divided into phosphatidylcholine (PC), phosphatidylethanolamine (PE), phosphatidylserine (PS), phosphatidylinositol (PI), phosphatidylglycerol (PG), glycerophosphatidic acid (PA), and so forth. From the perspective of the bond (ester, alkanoyl, or alkenoyl bond) between the fatty acid chain and glycerol skeleton at Sn-1 and Sn-2 (unsaturated) positions, the lipids can be divided into certain subclasses. Different types of phospholipids usually co-exist but the different polar heads determine that they cannot be detected simultaneously with the same detection mode. For example, PC and PS are subject to positive ionization, while PE, PI, PA, and PG are subject to negative ionization.
(4) The lipids with different structures are distinctly contained in biological tissues.

These characteristics of lipids require specific MALDI matrix systems. Cinnamic acid derivatives such as erucic acid (SA), α-cyano-4-hydroxycinnamic acid (HCCA), and benzoic acid derivatives such as 2,5-dihydroxybenzoic acid (DHB) are the earliest matrix for phospholipid analysis. 2,6-Dihydroxyacetophenone (DHA) is the most common neutral matrix. Correspondingly, 50–70% ethanol or methanol solutions (aq) containing 0.1% TFA are the most common solvents. The addition of cesium iodide [46] or lithium chloride [47] as the ionization reagent is conducive to MS analysis. 9-Aminoacridine (9-AA) was first adopted by Vermillion Salsbury and Hercules in the year 2002 to detect metabolites or phospholipids in peptide hydrolysates [48]. During the determination of lipids, cholesterol and triacylglycerides could not be ionized in the presence of 9-AA, and thereby the analysis complexity of phospholipids in lipids could be effectively reduced [49].

Metal and metal-oxide nanoparticles include Au, Ag, Mn, Zn, Fe_2O_3, TiO_2, ZnO, etc. For example, Jackson et al. sprayed gold colloid (5.5 nm) dispersed in ethanol with an artificial spray gun on rat brain slices for the determination of cerebroside [50]. Taira et al. modified two hematite (Fe_2O_3) unit cells (corundum-structured) with functionalized silicate materials to obtain functionalized nanoparticles (fNPs), and sprayed the fNPs on rat brain slices for the analysis of peptides and lipids [51].

The traditional analytical methods, such as HPLC, TLC, and GC-MS, are complicated and insensitive. For instance, for GC-MS analysis, phospholipids should be hydrolyzed first and then derivatized. Moreover, only the structures of fatty acyl groups can be recognized, and those of phospholipids cannot be accurately identified. HPLC-ESI-MS and ESI-MS techniques possess the merits of simple sample pretreatment, high resolution, easy automation, and so on. Liquid chromatography coupled with mass spectrometry (LC-MS) has greatly promoted the development of phospholipids, and the core technology is ESI-MS. The chromatographic technology strengthens the separation of phospholipids in samples, so the separation and identification process of phospholipids has the advantages of high throughput, high sensitivity, and efficiency. Phospholipids can be divided into glycerophospholipids and sphingomyelins (SM) according to their alcohol domains. Glycerophospholipids can be divided into PC, PE, PS, PI, PG, and PA according to the polar head. The ionization energy of MALDI MS is relatively high, so some samples that are insoluble in highly polar solvents such as methanol and water can also be ionized. In addition, this technique can deal with different types of lipids through rapid, sensitive, and high-throughput qualitative or quantitative analysis without special treatment.

TiO_2 has many good features including being nontoxic, no-scent, environmentally friendly, anti-corrosion, photocatalytic, able to absorb UV light, and having a large specific surface area. Its even size helps the analytes form uniform crystals; TiO_2 itself does not generate jamming signals like other matrices [52,53].

In this paper, titanium dioxide nanoparticles (TiO_2 NPs) were used as the matrix in MALDI MS for lipids analysis [54], the methodology of which was studied. The feasibility of TiO_2 NPs matrix and the influences of matrix solvents, matrix compositions, and ionization reagents

on the analysis of lipid samples by MALDI MS were discussed.

2 Materials and methods

2.1 Materials and instruments

Titanium dioxide was purchased from Sigma-Aldrich (St. Louis, MO), Purity: 99.5% trace metals basis, Particle Size: <100 nm (BET), <50 nm (XRD). Solvents including methanol and chloroform were purchased from Beijing Chemical Plant. Ultrapure water was self-made with a Milli Q machine. Anhydrous ethanol was provided by the Institute of Chemistry, Chinese Academy of Sciences. The ionization reagent NaCl was purchased from Beijing Chemical Plant. Biological small molecules including Y-aminobutyric acid, taurine, 3,4-dihydroxybenzene acetic acid, vitamin C, hypoxanthine nucleoside, xanthine, hypoxanthine, homovanillic acid, cytosine nucleoside, creatinine, isoprenaline hydrochloride, adenosine-5-monophosphate disodium salt, uridine, acetylcholine chloride, adenine, and guanine nucleoside were provided by the Institute of Chemistry, Chinese Academy of Sciences. Lipid standards including gangliosides GM1 ($C_{73}H_{131}N_3O_{31}$), (3-dodecanoyloxy-2-hydroxypropyl)2-(trimethylazaniumyl)ethyl phosphate 12:0 LPC ($C_{20}H_{42}NO_7P$), 12:0 ceramide ($C_{30}H_{59}NO_3$), L-alpha-lysophosphatidylcholine 16:0 LPC ($C_{24}H_{50}NO_7P$), 1-hexadecanoyl-2-(9*Z*-octadecenoyl)-*sn*-glycerol 16:0–18:1 DG ($C_{37}H_{70}O_5$), *N*-heptadecanoyl-D-erythro-sphingosylphosphorylcholine 17:0 SM ($C_{40}H_{81}N_2O_6$), 18:1–12:0 glucosyl(β)ceramide ($C_{36}H_{69}NO_8$), 1-hexadecanoyl-2,3-di-(9*Z*-octadecenoyl)-*sn*-glycerol 18:1–16:0–18:1TG ($C_{55}H_{102}O_6$), 1,2-distearoyl-*sn*-glycero-3-phosphate 18:0 PA ($C_{39}H_{77}O_8P$), *N*-nervonoyl-D-erythro-sphingosylphosphorylcholine 24:1 SM ($C_{47}H_{93}N_2O_6P$), cholesterol-d7 ($C_{27}H_{39}OD_7$), galactosylceramide d-G1-cer ($C_{36}H_{69}NO_8$), lactosyl(β)ceramide ($C_{42}H_{79}NO_{13}$), *N*-[(2*S*,3*R*)-1,3-dihydroxyoctadecan-2-yl]-2-hydroxyhexadecanamide (d16:0/18:0, Cer), 17:0 ceramide ($C_{35}H_{69}NO_3$), *N*-oleoyl-D-erythro- sphingosylphosphorylcholine 18:1 SM ($C_{41}H_{81}N_2O_6P$), [(2*R*)-3-[2-aminoethoxy (hydroxy)phosphoryl]oxy-2-hydroxypropyl] dodecanoate 16:0, and LPE ($C_{21}H_{44}NO_7P$) were provided by the Chinese Academy of Sciences Chemistry. 1-Myristoyl-2-hydroxy-*sn*-glycero-3-phosphate 14:0 LPA ($C_{17}H_{35}NO_7P$), 1,2-dinonadecanoyl-*sn*-glycero-3-phosphocholine 19:0 PC ($C_{46}H_{92}NO_8P$), and 1-*O*-hexadec-1′-enyl-2-eicosatetraenoyl-PE 17:0 PE ($C_{39}H_{78}NO_8P$) were purchased from Beijing Shennongyuan Biotechnology Development Co., Ltd. Samples of mixed lipids were extracted from the brain homogenate with methanol alone and with a Bligh & Dyer method [55,56], separately. An analytical balance, pipettes, and 50 mL beakers were employed. A Solarix ft ms spectrometer was used in the determination and the parameters of the mass spectrometer are listed in Table 1.

2.2 Preparation of samples, matrix, and ionization reagents

A matrix solution was prepared as follows: 1 mg of titanium dioxide was mixed with 1 mL of absolute ethanol. An ionization reagent was prepared as follows: sodium chloride was dissolved in absolute ethanol to form a 10^{-5} mol·L^{-1} solution.

Biological small-molecule solutions were prepared as follows: a sample was mixed with absolute ethanol to prepare 0.1 mL of a 0.001 mol·L^{-1} solution.

A lipid standard solution was prepared as follows: a standard was mixed with 1 mL of methanol, and 0.1 mL of the solution was withdrawn as a 0.001 mol·L^{-1} lipid standard solution.

A solution of mixed lipids was prepared as follows: 1 mL methanol was added to the mixed lipids, and 0.1 mL of the solution was withdrawn as a 0.001 mol·L^{-1} solution of mixed lipids.

2.3 Pretreatment of samples of mixed lipids

Two methods were separately applied for the pretreatment: the method using methanol alone and the B&D method.

The former method was performed as follows: 450 µL of methanol was mixed with 50 µL of the brain homogenate. After stirring for 1 min, the mixture was placed for 30 s and then was centrifuged for 10 min at 12,000 rpm. 100 µL of the extract was withdrawn with a pipette and

Table 1: Parameters of the mass spectrometer

Name	Solarix ft ms
Range of *m/z*	100–10,000
Function	Series connection
Resolution	10,000,000
Error of precise *m/z* value	<600 ppb (RMS)
Sensitivity	S/N > 10:1 < 100 amol
Switching speed between positive and negative values	4 H

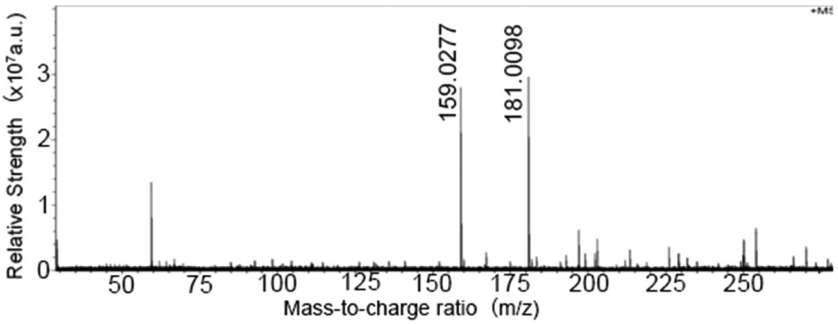

Figure 1: The mass spectrum of hypoxanthine with methanol as the solvent.

stored at −20°C (the sample contained lipids after the removal of proteins and minerals).

The B&D method was performed as follows: 250 µL of chloroform and 500 µL of methanol were mixed as the solvent. About 100 µL of the brain homogenate was mixed with the solvent, and the mixture was stored at −20°C for 5 min with ice. Then, 250 µL of water and 250 µL of chloroform were added. After stirring for 1 min, the mixture was centrifuged for 10 min at 12,000 rpm. Then, 100 µL of the extracts at upper and lower layers were separately withdrawn and stored at −20°C, separately (the samples contained different lipids with different molecular polarities after the removal of proteins and minerals).

2.4 Preparation of MALDI samples

With TiO_2 as the matrix, all the samples for analysis were prepared with a dry-point method implemented as follows: 3 µL of a sample solution and 3 µL of the matrix solution were uniformly mixed. If an ionization reagent was required, 1 µL of a sodium chloride solution was added to the mixture. After complete mixing, 1 µL of the mixture was added dropwise on a clean stainless-steel sample target. After the evaporation of solvent and crystallization of the sample, a qualified sample was thus prepared for analysis with the mass spectrometer.

3 Result and discussion

3.1 Influence of TiO_2 matrix solvent

Water, absolute ethanol, and methanol were separately used as the solvent to prepare a matrix solution for the detection of small biological molecules. When water was used as the solvent, a suspension was formed, and the sites with concentrated samples were difficult to find, so water serving as the solvent was denied. Figures 1 and 2 show the spectra with methanol and anhydrous ethanol as the matrix solvent, respectively. After comparison, the signals in Figure 1 were distributed disorderly and contained many signals of impurities. Therefore, absolute ethanol was chosen as the solvent, and TiO_2 was chosen as the matrix for determination; the results showed clearer signals, compared with those in Figures 1 and 2, even if the spectra were of 10^{-7} and 10^{-8}, the signal peaks obtained by MS can be clearly separated. These spectral results show that the detection precision was high with the use of the TiO_2 matrix and absolute ethanol solvent. The precision of MS for solvent is good.

3.2 Influence of the TiO_2 matrix concentration

About 0.01, 0.1, 1, and 10 mg of TiO_2 were separately used for the preparation of matrix solutions for the determination

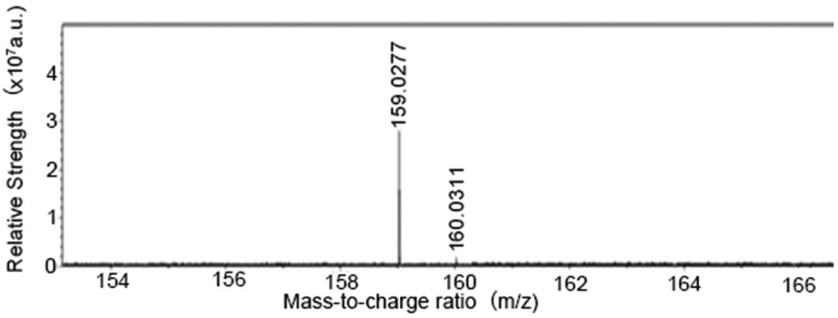

Figure 2: The mass spectrum of hypoxanthine with ethanol as the solvent.

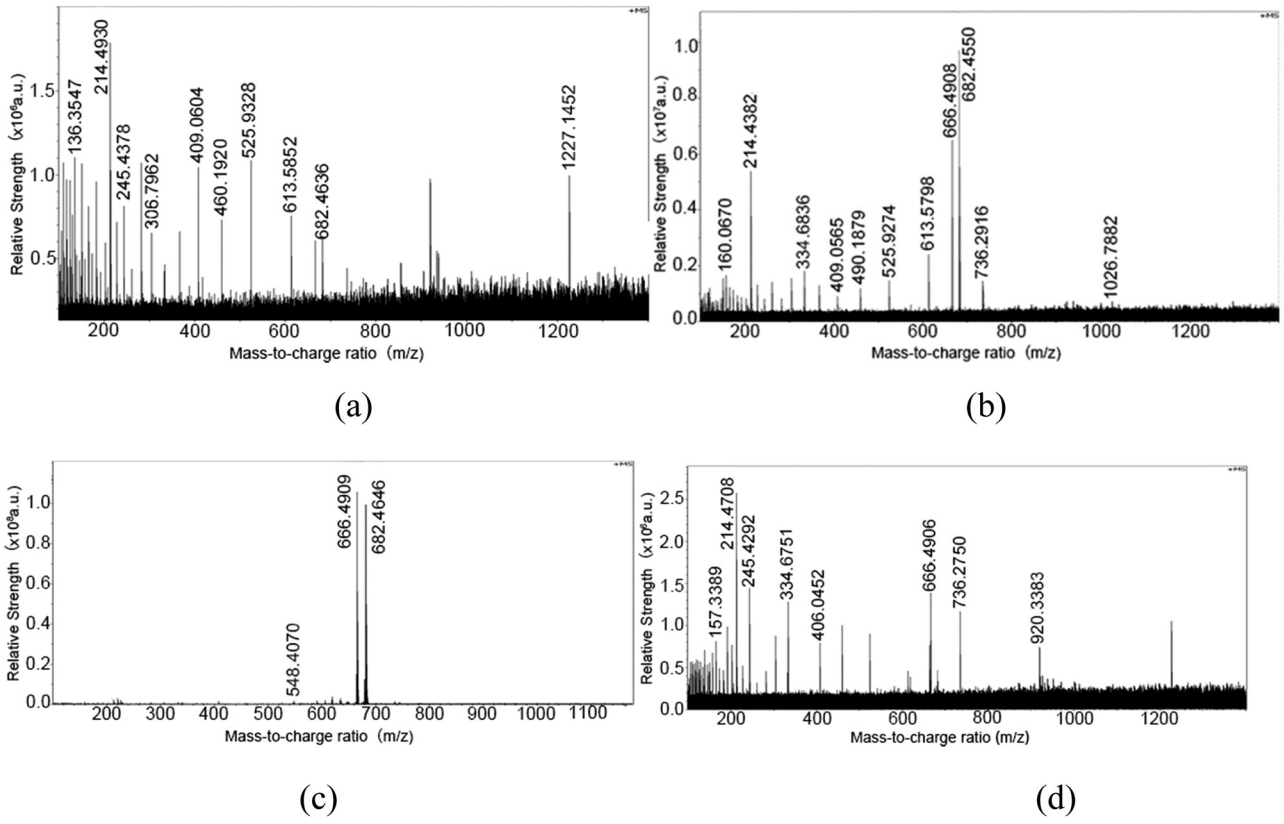

Figure 3: The mass spectrum of GC under the conditions of (a) 0.01 mg, (b) 0.1 mg, (c) 1 mg, and (d) 10 mg of TiO_2.

of 18:1–12:0 glucosyl(β)ceramide (GC, $C_{36}H_{69}NO_8$). The resulting mass spectra with different TiO_2 concentrations were compared for the optimization of the TiO_2 content.

Figure 3 shows that the mass spectra of 18:1–12:0 glucosyl(β)ceramide (GC, $C_{36}H_{69}NO_8$) obtained under the conditions of these four concentrations are rather different. The mass spectrum under the condition of 1 mg of TiO_2 is the clearest, almost without interfering signals, which can be seen from Figure 3c. In contrast, the other three spectra contain intense interfering signals and show poor results. Hence, 1 mg of matrix per mL was selected in the following experiment.

3.3 Influence of ionization reagents

Li^+, Na^+, K^+, and Se^+ were separately selected as the ionization reagent in the determination of 18:1–12:0 glucosyl(β)ceramide (GC, $C_{36}H_{69}NO_8$). The resulting mass spectra were compared for the optimization of the ionization reagent in this experiment.

Figure 4 shows that the mass spectra of 18:1–12:0 glucosyl(β)ceramide (GC, $C_{36}H_{69}NO_8$) separately obtained in the presence of these four ionization reagents are distinct. Among them, the spectrum in the presence of Na^+ is the clearest, almost without interfering signals, which can be seen from Figure 4c. In contrast, the other three spectra contain intense interfering signals and exhibit poor quality. Hence, NaCl was selected as the ionization reagent in the following experiment.

3.4 Influence of option between positive and negative MS

The mixed lipids samples are usually extracted from plasma, brain homogenate, and so forth. In the present work, lipids were extracted with methanol alone and the B&D method, separately. The former lipids extracted seemed like lipids. The latter seemed like samples with high polarity and small polarity. The volumetric ratio of plasma to methanol in the former method was 1:9. The volumetric ratio of methanol/chloroform/water in the B&D method was 1:1:0.9. The positive and negative mass spectra of samples extracted by both methods were compared.

The negative mass spectra shown in Figure 6 were compared with the positive spectra shown in Figure 5, respectively. It was found that the interfering signals of

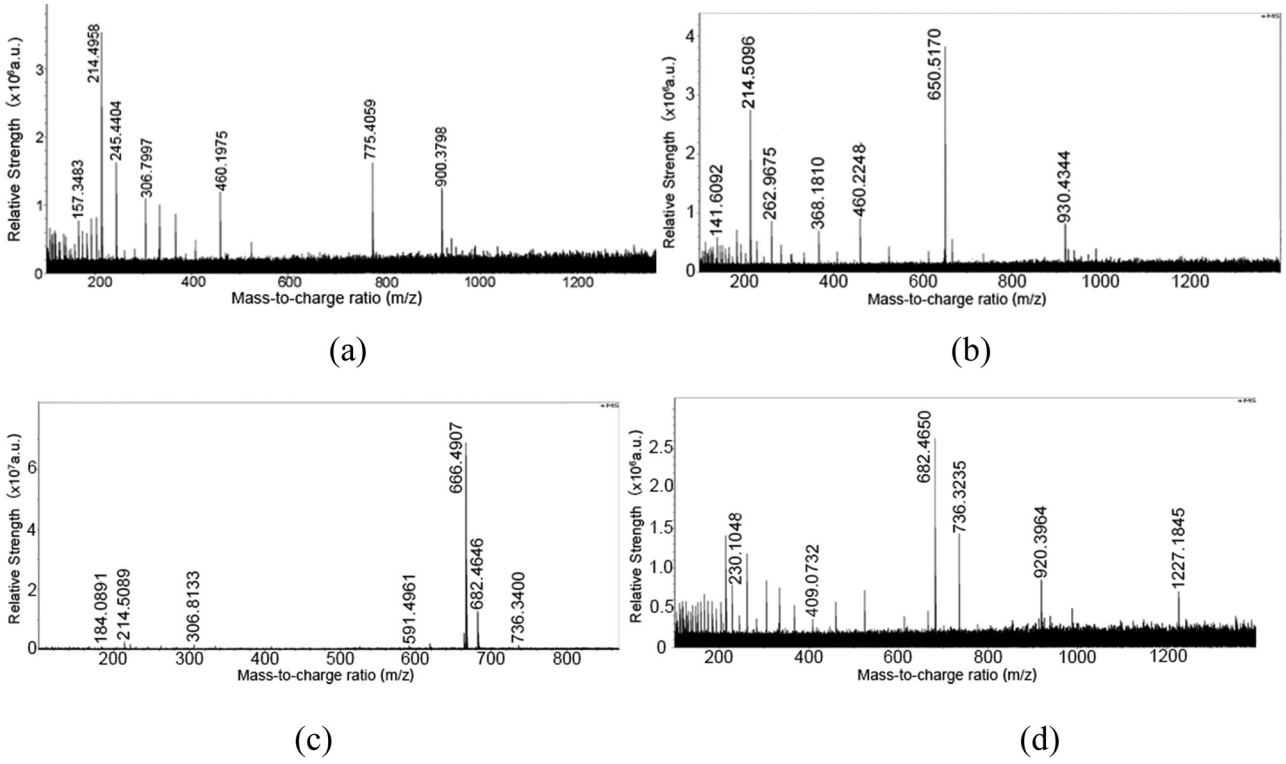

Figure 4: The spectrum of GC in the presence of ionization reagents: (a) Se^+, (b) Li^+, (c) Na^+ (C), and (d) K^+.

the positive spectra were far less than those of the negative spectra. Figure 5 shows that the positive mass spectra of lipids, whether a high or low polarity, exhibit clear signals. On the other hand, the positive and negative mass spectra of samples extracted with methanol alone show similar graphic quality (see Figure 7). In summary, positive MS was selected in the following sections.

The positive and negative mass spectra of samples extracted with the B&D method (upper and lower layers) and methanol alone are illustrated as follows: the B&D method in Figures 5 and 6 and the extraction with methanol alone in Figure 7.

3.5 Mass spectra of lipid standards

The lipid standards were determined with 1 mg of TiO_2 as the matrix, absolute ethanol as the solvent, and NaCl as the ionization reagent. The corresponding mass spectra were obtained.

Under the conditions of absolute ethanol as the matrix solvent, 1 mg of the matrix, and Na^+ as the ionization reagent, the mass spectra of lipid standards were almost clear with a few interfering signals, which did not appreciably interfere with the signals of lipid standards. TiO_2 predominantly detected $[M]^+$, $[M + H]^+$,

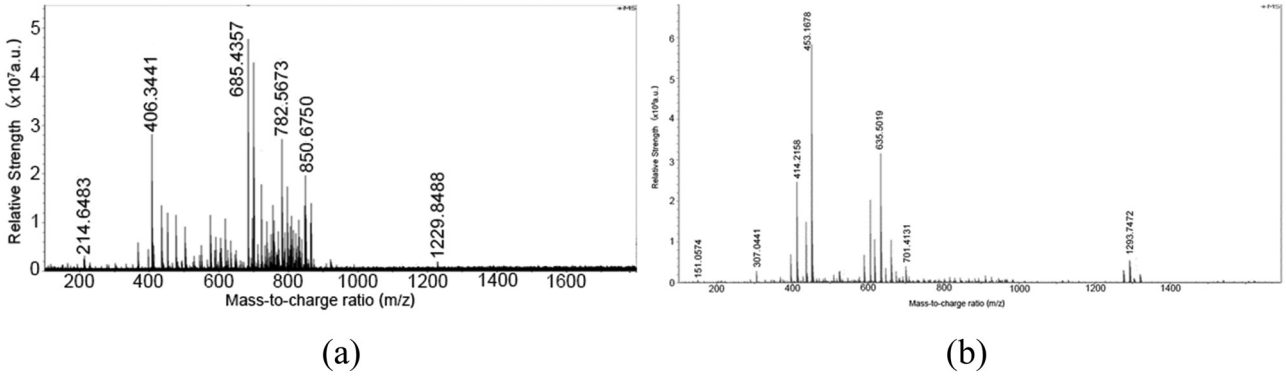

Figure 5: The positive mass spectrum of the lower layer (a) and the upper layer (b) of the sample extracted with the B&D method.

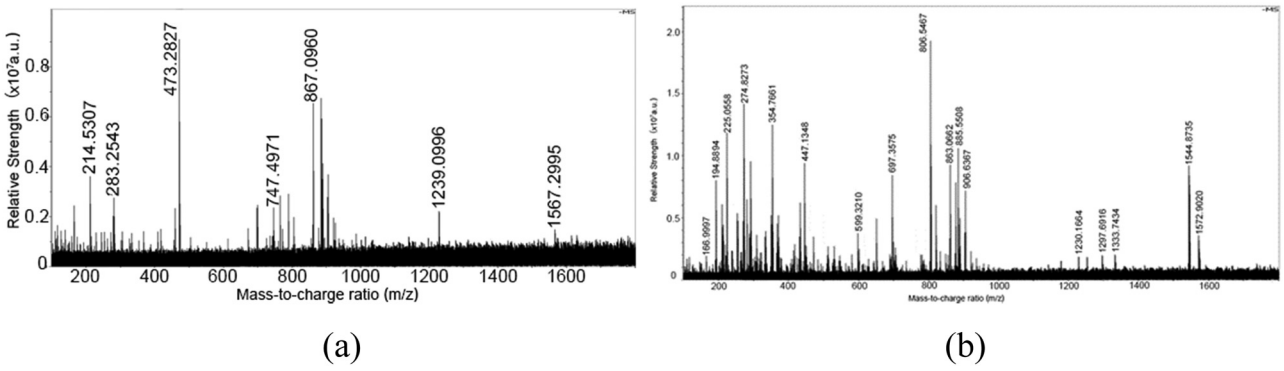

Figure 6: The negative mass spectrum of the lower layer (a) and the upper layer (b) of the sample extracted with the B&D method.

$[M + Na]^+$, and $[M + K]^+$ ions. The mass spectra of GM, ceramide, GC, TG, PC, and PE show clear signals with a few interfering signals by using TiO_2 as the matrix for MS. In particular, the conventional organic matrix (cyano-4-hydroxycinnamic acid, CCA) and TiO_2 as the matrix for comparison of MS are shown in Figure 8, and the spectrum of ceramide using titanium dioxide matrix is very clear. However, for the DHB-based TOF MS measurements, some of the galactocerebroside peaks overlap with the PC peaks with the mass resolution of measurements [57]. The information on lipid standards is shown in Table 2.

MALDI MS is a soft ionization technique. Its traditional matrices create massive interference when the sample has a low mass-to-charge ratio, which makes it difficult to analyze small molecules. Comparing with a small organic molecular matrix, TiO_2 NPs perform very well at a low m/z (<500 Da) interval. Moreover, the structure of TiO_2 NP crystals is uniform that improves the reproducibility, stability, and sensitivity of the analytical

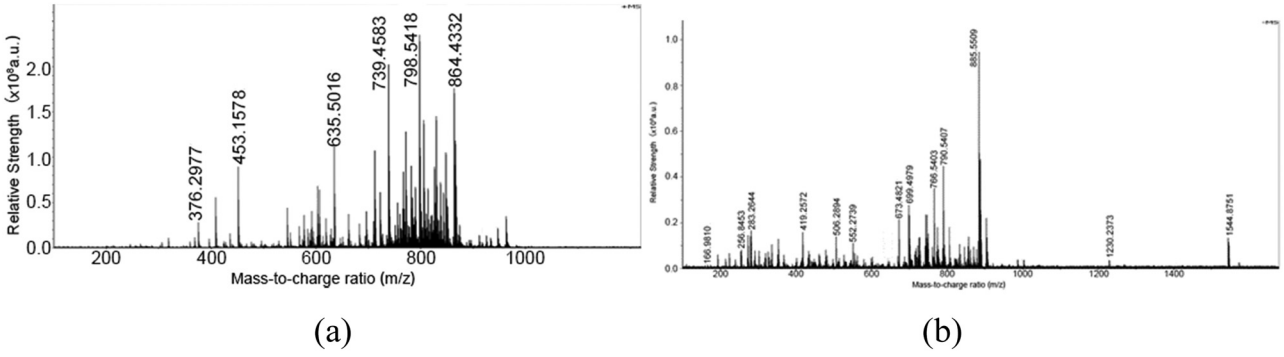

Figure 7: The positive mass spectrum (a) and the negative mass spectrum (b) of the sample extracted with methanol alone.

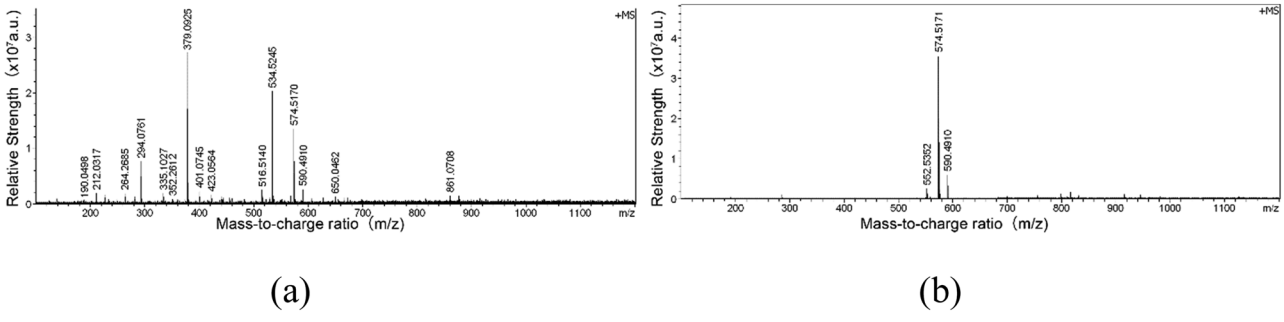

Figure 8: The mass spectrum of 17:0 ceramide by CCA (a) and TiO_2 (b) as the matrix.

Table 2: Information of lipid standards

Sample	$[M]^+$ *m/z*	$[M + H]^+$ *m/z*	$[M + Na]^+$ *m/z*	$[M + K]^+$ *m/z*	Sensitivity (ppm)
GM1	1545.8761	1546.8839	1568.5972	1584.5711	0.14
12:0 LPC	439.2772	440.2850	462.2591	478.2331	0.31
12:0 ceramide	481.4490	482.4568	504.4387	520.4127	0.12
16:0 LPC	495.3319	496.3398	518.3217	534.2957	0.14
16:0–18:1 DG	594.5218	595.5296	617.5116	633.4855	0.25
17:0 SM	716.5827	717.5905	739.5725	755.5464	0.26
18:1–12:0 GC	643.5018	644.5096	666.4915	682.4655	0.12
18:1–16:0 TG	858.7671	859.7749	881.7569	897.7308	0.11
18:0 PA	704.5272	705.5351	727.5248	743.4988	0.34
24:1 SM	812.6766	813.6844	835.6664	851.6403	0.21
Cholesterol-d7	393.3983	394.4061	416.3880	432.3620	0.28
d-G1-cer	643.5018	644.5096	666.4915	682.4655	0.35
Lactosyl(β)cer	805.5546	806.5625	828.5444	844.5183	0.31
17:0 ceramide	551.5272	552.5350	574.5170	590.4909	0.10
18:1 SM	728.5827	729.5905	751.5725	767.5464	0.25
16:0 LPE	453.2850	454.2929	476.2748	492.2487	0.33
17:0 PE	719.5460	720.5538	742.5357	758.5097	0.13
19:0 PC	817.6555	818.6633	840.6453	856.6192	0.17

$[M]^+$: The molecular ion of the sample.
$[M + H]^+$: The molecular ion of the sample adsorbing hydrogen ions.
$[M + Na]^+$: The molecular ion of the sample adsorbing sodium ions.
$[M + K]^+$: The molecular ion of the sample adsorbing potassium ions.
The numbers listed in the table are the molecular weights of the corresponding compounds in different ionic states.

method. In conclusion, TiO_2 NPs have great advantages as a matrix in lipidomics studies.

4 Conclusion

Lipids with diverse structures possess many biological functions and play an indispensable role not only in the regulations of various physiological activities (energy conversion, materials transport, information recognition and transmission, cells development, differentiation, and apoptosis). MS has been widely applied because of its high sensitivity, specificity, high throughput, and high accuracy.

In this study, FT-ICR-MS was used as the instrument for the determination of small biological molecules (such as hypoxanthine, guanosine, uridine, and cytidine), lipid standards (such as GC, GM, SM, PE, PC, and ceramide), and mixed lipids in the mode of positive MS, with TiO_2 as the matrix, absolute ethanol as the matrix solvent (a matrix solution was prepared by dissolving TiO_2 in absolute ethanol), 1 mg·mL^{-1} matrix, and NaCl as the ionization reagent. The spectra derived showed clear signals, good sensitivity, and a few interfering signals.

As a new matrix for MALDI MS, TiO_2 NPs explore the possible applications of inorganic matrices instead of traditional organic matrices. There are several points regarding TiO_2 NPs as a matrix and should be further studied. The first goal is to improving TiO_2 NPs to work for other types of analytes. Second, experiments show that the crystallization type of the matrix and the analyte has strong effects on the result, yet there is no theoretical basis or explanation for this phenomenon. This makes it difficult to make qualitative and quantitative analyses, so a theoretical basis will have a significant impact. Last, but not least, the features of TiO_2 NPs make it a potential matrix for imaging MS.

Funding information: This research was financially supported by the National Natural Science Foundation of China (Grants No. 11475020 and 11975048) and Beijing Union University Graduate Program.

Author contributions: Congnan Peng: writing – original draft, Qian Zhang: writing – review and editing, Jian-an Liu: data curation, Zhen-peng Wang: methodology, formal analysis; Zhen-wen Zhao: funding acquisition; Ning Kang and Yuxin Chen: validation, Qing Huo: supervision, conceptualization.

Conflict of interest: The authors state no conflict of interest.

References

[1] Saul Y, Miron K, Yuval C, Roderick J. Treatment of inflammatory diseases by selective eicosanoid inhibition: a double-edged sword. Trends Pharmacol Sci. 2007;28(9):459–64. doi: 10.1016/j.tips.2007.07.005.

[2] Léon J, Rob F, Ben J, Jacques J, Jo G, Erik S, et al. Hypertension is associated with marked alterations in sphingolipid biology: a potential role for ceramide. PLoS One. 2011;6(7):e21817. doi: 10.1371/journal.pone.0021817.

[3] Fumiaki I, Yoko S, Tomoyuki I. Measurement and clinical significance of lipid peroxidation as a biomarker of oxidative stress: oxidative stress in diabetes, atherosclerosis, and chronic inflammation. Antioxidants. 2019;8(72):1–28. doi: 10.3390/antiox8030072.

[4] Ungaro F, Rubbino F, Danese S, D'Alessio S. Actors and factors in the resolution of intestinal inflammation: lipid mediators as a new approach to therapy in inflammatory bowel diseases. Front Immunol. 2017;8:1331–1. doi: 10.3389/fimmu.2017.01331.

[5] Eoin F, Shankar S, Christian R, Christopher K, Alfred H, Robert C, et al. A comprehensive classification system for lipids. J Lipid Res. 2005;46(5):839–62. doi: 10.1194/jlr.E400004-JLR200.

[6] Joseph C. Thin-layer chromatographic procedures for lipid separation. J Chromatogr B. 1995;671(1–2):169–95. doi: 10.1016/0378-4347(95)00232-8.

[7] Ruth W, Wang XM. Lipid species profiling: a high-throughput approach to identify lipid compositional changes and determine the function of genes involved in lipid metabolism and signaling. Curr Opin Plant Biol. 2004;7(3):337–44. doi: 10.1016/j.pbi.2004.03.011.

[8] Richard H, Edward A. Applications of mass spectrometry to lipids and membranes. Annu Rev Biochem. 2011;80(1):301–25. doi: 10.1146/annurev-biochem-060409-092612.

[9] Hanan F, Carisa C, Franklin W, editors. Warf: lipids by nuclear magnetic resonance (NMR) spectroscopy. Poster; 2019 Aug; doi: 10.13140/RG.2.2.28959.38561. Availble from: https://www.researchgate.net/publication/337495086.

[10] Kim HY, Salem N. Liquid chromatography-mass spectrometry of lipids. Prog Lipid Res. 1993;32(3):221–45. doi: 10.1016/0163-7827(93)90008-K.

[11] Tânia M, Javier-Fernando M, Pedro D, Rosário D. Discovery of bioactive nitrated lipids and nitro-lipid-protein adducts using mass spectrometry-based approaches. Redox Biol. 2019;10(2):1–16. doi: 10.1016/j.redox.2019.101106.

[12] Chen ZC. Progress in the effects of omega-3 fatty acids on brain and cardiovascular system. Her Med. 2013;32(10):1. doi: CNKI:SUN:YYDB.0.2013-10-057.

[13] Liu TT, Cui DH. Role of lipids and lipid-associated proteins in Alzheimer's disease. J Neurosci Ment Health. 2008;8(5):329–34. doi: 10.3969/j.issn.1009-6574.2008.05.001.

[14] Marta L. Fat diet helps brain health. Swine Prod. 2014;1:23–3. doi: 10.3969/j.issn.1002-1957.2014.01.008.

[15] Sun RY, Ge JY, Zhang Y, Li P, Yang H, Li B. Study on the changes of lipid distribution in the brain of mice with ischemic stroke based on MALDI mass spectrometry. CMSC. 2018;316. doi: 10.26914/c.cnkihy.2018.013401.

[16] Wan XL, Xia XH, Liu M, Zhang CF. The correlation between the fatty acids metabolism and ischemia stroke based on metabolomics. Guangdong Med J. 2014;35(24):3788–91. doi: 10.13820/j.cnki.gdyx.2014.24.006.

[17] Alan G, Christopher L. Fourier transform ion cyclotron resonance detection: Principles and experimental configurations. Int J Mass Spectrom. 2002;215(1–3):59–75. doi: 10.1016/S1387-3806(01)00588-7.

[18] Cuong H, Jun H, Christoph H. Dithranol as a MALDI matrix for tissue imaging of lipids by fourier transform ion cyclotron resonance mass spectrometry. Anal Chem. 2012;84(19):8391–8. doi: 10.1021/ac301901s.

[19] Beate F, Kristin B, Jürgen S. Oxidative changes of lipids monitored by MALDI MS. Chem Phys Lipids. 2011;164(8):782–95. doi: 10.1016/j.chemphyslip.2011.09.006.

[20] Melvin B, Joe D. Error estimates for finite zero-filling in Fourier transform spectrometry. Anal Chem. 1979;51(13):2198–203. doi: 10.1021/ac50049a032.

[21] Renato Z, Richard K. Ion formation in MALDI mass spectrometry. Mass Spectr Rev. 1998;17(5):337–66. doi: 10.1002/(SICI)1098-2787(1998)17:5<337:AID-MAS2>3.0.CO;2-S.

[22] Distler A, Allison J. Improved MALDI-MS analysis of oligonucleotides through the use of fucose as a matric additive. Anal Chem. 2001;73(20):5000–3. doi: 10.1021/ac015550+.

[23] Beate F, Jürgen S, Rosmarie S, Matthias Z, Augustinus B, Peter M, et al. Analysis of stem cell lipids by offline HPTLC-MALDI-TOF MS. Anal Bioanal Chem. 2008;392(5):849–60. doi: 10.1007/s00216-008-2301-8.

[24] Li LX, Zhong SS, Shen X, Li QJ, Xu WX, Tao YZ, et al. Recent development on liquid chromatography-mass spectrometry analysis of oxidized lipids. Free Radic Bio Med. 2019;144:16–34. doi: 10.1016/j.freeradbiomed.2019.06.006.

[25] Wei H, Kerstin N, David H, James H, Mei-Chuan K, Robert T. Electrospray sample deposition for matrix-assisted laser desorption/ionization (MALDI) and atmospheric pressure MALDI mass spectrometry with attomole detection limits. Rapid Commun Mass Spectrom. 2004;18(11):1193–200. doi: 10.1002/rcm.1458.

[26] Hoa T, Kyu H, Woong J, Hyung S, Tae W. Combination of microwave-assisted Girard derivatization with ionic liquid matrix for sensitive MALDI-TOF MS analysis of human serum N-glycans. J Anal Methods Chem. 2018;2018:1–7. doi: 10.1155/2018/7832987.

[27] Yang YC, Chen QF, Xia Y. Research progress in novel matrixes for MALDI—TOF MS analysis of small molecule compounds. J Instrum Anal. 2018;37(11):1381–7. doi: 10.3969/j.issn.1004-4957.2018.11.018.

[28] Mock K, Sutton C, Cottrell J. Sample immobilization protocols for matrix-assisted laser-desorption mass spectrometry. Rapid Commun Mass Spectrom. 1992;6(4):233–8. doi: 10.1002/rcm.1290060402

[29] Randall W, David D, Peter W. Determination of human IGM at m/z-similar-to-1MDa. Rapid Commun Mass Spectrom. 1995;9(7):625–5. doi: 10.1002/rcm.1290090717.

[30] Kenneth N, Rory T, Josephine B. Matrix optical absorption in UV-MALDI MS. J Am Soc Mass Spectr. 2017;29(3):501–11. doi: 10.1007/s13361-017-1843-4.
[31] Alireza B, Seth W, Masoud Z, Ahmed H, Yehia M. Magnetic carbon nanocomposites as a MALDI co-matrix enhancing MS-based glycomics. Anal Bioanal Chem. 2018;410(28):7395–404. doi: 10.1007/s00216-018-1345-7.
[32] Ding F, Qian Y, Deng ZA, Zhang JT, Zhou YC, Yang L, et al. Size-selected silver nanoparticles for MALDI-TOF mass spectrometry of amyloid-beta peptides. Nanoscale. 2018;10(6):22044–54. doi: 10.1039/C8NR07921H.
[33] Chen SM, Zheng HZ, Wang JN, Hou J, He Q. Carbon nanodots as a matrix for the analysis of low-molecular-weight molecules in both positive- and negative-ion matrix-assisted laser desorption/ionization time-of-flight mass spectrometry and quantification of glucose and uric acid in real samples. Anal Chem. 2013;85(14):6646–52. doi: 10.1021/ac401601r.
[34] Wang S, Niu H, Zeng T, Zhang X, Cao D. Rapid determination of small molecule pollutants using metal-organic frameworks as adsorbent and matrix of MALDI-TOF-MS. Micropor Mesopor Mater. 2017;239:390–5. doi: 10.1016/j.micromeso.2016.10.032.
[35] Chen LF, Ou JJ, Wang HW, Liu ZS, Ye ML. Tailor-made stable Zr(IV)-based metal–organic frameworks for laser desorption/ionization mass spectrometry analysis of small molecules and simultaneous enrichment of phosphopeptides. ACS Appl Mater Interfaces. 2016;8(31):20292–300. doi: 10.1021/acsami.6b06225.
[36] Han GB, Zeng QL, Jiang ZW, Xing TT, Huang CZ. MIL-101(Cr) as matrix for sensitive detection of quercetin by matrix-assisted laser desorption/ionization mass spectrometry. Talanta. 2017;164:355–61. doi: 10.1016/j.talanta.2016.11.044.
[37] Lu MH, Lai YQ, Chen GN, Cai ZW. Matrix interference-free method for the analysis of small molecules by using negative ion laser desorption/ionization on graphene flakes. Anal Chem. 2011;83:3161–9. doi: 10.1021/ac2002559.
[38] Abdelhami H, Wu BS, Wu HF. Graphene coated silica applied for high ionization matrix assisted laser desorption/ionization mass spectrometry: a novel approach for environmental and biomolecule analysis. Talanta. 2014;126:27–37. doi: 10.1016/j.talanta.2014.03.016.
[39] Min QH, Zhang XX, Chen XQ, Li SY, Zhu JJ. N-Doped Graphene: an alternative carbon-based matrix for highly efficient detection of small molecules by negative ion MALDI-TOF MS. Anal Chem. 2014;86:9122–30. doi: 10.1021/ac501943n.
[40] Shi CY, Deng CH. Recent advances in inorganic materials for LDI-MS analysis of small molecules. Analyst. 2016;141:2816–26. doi: 10.1039/c6an00220j.
[41] Lin ZA, Zheng JN, Lin G, Tang Z, Yang XQ. Negative ion laser desorption/ionization time-of-flight mass spectrometric analysis of small molecules using graphitic carbon nitride nanosheet matrix. Anal Chem. 2015;87:8005–12. doi: 10.1021/acs.analchem.5b02066.
[42] Li X, Chen XM, Tan J, Liang X, Wu JM. Palladium modified porous silicon as multifunctional MALDI chip for serum peptide detection. Analyst. 2017;142:586. doi: 10.1039/c6an02165d.
[43] Wei JY, Zhang YJ, Tan F, Liu HL, Wang JL. A novel desalting method on target for MALDI-TOF-MS analysis based on Fe3O4/TIO2 nanoparticles. Chin J Anal Chem. 2007;1:1–7. doi: 10.3321/j.issn:0253-3820.2007.01.001.
[44] Yang MR, Wang M, Tang XY, Zhou J, Mao XF. Analysis of small molecule compounds by matrix assisted laser desorption ionization time-of-flight mass spectrometry with ZnO, CuO and NiO nanoparticles as matrix. Chin J Anal Chem. 2015;43:1058–62. doi: CNKI:SUN:FXHX.0.2015-07-021.
[45] He Q, Chen SM, Wang JN, Hou J, Wang JY. 1-Naphthylhydrazine hydrochloride: a new matrix for the quantification of glucose and homogentisic acid in real samples by MALDI-TOF MS. Clin Chim Acta. 2013;420:94–8. doi: 10.1016/j.cca.2012.10.015.
[46] Wang HJ, Jackson S, Woods A. Direct MALDI-MS analysis of cardiolipin from rat organs sections. J Am Soc Mass Spectrom. 2007;18(3):567–77. doi: 10.1016/j.jasms.2006.10.023.
[47] Jackson S, Wang HJ, Woods A. In situ structural characterization of phosphatidylcholines in brain tissue using MALDI-MS/MS. J Am Soc Mass Spectrom. 2005;16(12):2052–6. doi: 10.1016/j.jasms.2005.08.014.
[48] Vermillion-Salsbury R, Hercules D. 9-Aminoacridine as a matrix for negative mode matrix-assisted laser desorption/ionization. Rapid Commun Mass Spectrom. 2002;16(16):1575–81. doi: 10.1002/rcm.750.
[49] Sun G, Yang K, Zhao Z, Guan S, Han X. Matrix-assisted laser desorption/ionization time-of-flight mass spectrometric analysis of cellular glycerophospholipids enabled by multiplexed solvent dependent analyte-matrix interactions. Anal Chem. 2008;80(19):7576–85. doi: 10.1021/ac801200w.
[50] Jackson S, Ugarov M, Egan T, Post J, Langlais D. MALDI-ion mobility-TOFMS imaging of lipids in rat brain tissue. J Mass Spectrom. 2007;42(8):1093–8. doi: 10.1002/jms.1245.
[51] Taira S, Sugiura Y, Moritake S, Shimma S, Ichiyanagi Y. Nanoparticle-assisted laser desorption/ionization based mass imaging with cellular resolution. Anal Chem. 2008;80(12):4761–6. doi: 10.1021/ac800081z.
[52] Machálková M, Schejbal J, Glatz Z, Preisler J. A label-free MALDI TOF MS-based method for studying the kinetics and inhibitor screening of the Alzheimer's disease drug target B-secretase. Anal Bioanal Chem. 2018;410(28):7441–8. doi: 10.1007/s00216-018-1354-6.
[53] Lou XW, Leenders C, Onzen A, Bovee R, Dongen J, Vekemans J, et al. False results caused by solvent impurity in tetrahydrofuran for MALDI TOF MS analysis of amines. J Am Soc Mass Spectrom. 2014;25(2):297–300. doi: 10.1007/s13361-013-0766-y.
[54] Wang H, Duan JC, Cheng Q. Photocatalytically patterned TiO_2 arrays for on-plate selective enrichment of phosphopeptides and direct MALDI MS analysis. Anal Chem. 2011;83(5):1624–31. doi: 10.1021/ac1024232.
[55] Ulmer C, Jones C, Yost R, Garrett T, Bowden J. Optimization of Folch, Bligh-Dyer, and Matyash sample-to-extraction solvent ratios for human plasma-based lipidomics studies. Anal Chim Acta. 2018;1037(11):351–7. doi: 10.1016/j.aca.2018.08.004.
[56] Ghosh R, Makam R, Krishnamurthy V, Siva Kiran RR. Ultrasonication assisted Bligh and dyer method for extraction of lipids from green algae. Asian J Chem. 2019;31(7):1555–7. doi: 10.14233/ajchem.2019.22033.
[57] Qian W, James LC, Stanislav SR, Martha UG, Jonathan VS. Dopamine-modified TiO_2 monolith-assisted LDI MS imaging for simultaneous localization of small metabolites and lipids in mouse brain tissue with enhanced detection selectivity and sensitivity. Chem Sci. 2017;8:3926–38. doi: 10.1039/c7sc00937b.